Quantification of Shape, Angularity, and Surface Texture of Base Course Materials

Vincent C. Janoo

January 1998

Abstract: A state-of-the-art review was conducted to determine existing test methods for characterizing the shape, angularity, and surface texture of coarse aggregates. The review found direct methods used by geologists to determine these characteristics. These methods involve physical measurements of individual aggregates and are very laborious and time consuming. Engineers have developed index tests (indirect methods) to quantify the combined effect of the shape, angularity, and surface texture of coarse aggregates in terms of changes in the voids in the aggregate bulk. A description of both the direct and indirect methods is provided in the report. Also, the effect of shape, angularity, and surface texture of coarse aggregates on the base course performance was reviewed. It was found that there is some contradiction in the published data on resilient modulus. Shape, angularity, and surface texture of coarse aggregates clearly influence the angle of internal friction.

How to get copies of CRREL technical publications:

Department of Defense personnel and contractors may order reports through the Defense Technical Information Center:

DTIC-BR SUITE 0944
8725 JOHN J KINGMAN RD
FT BELVOIR VA 22060-6218
Telephone 1 800 225 3842
E-mail help@dtic.mil
msorders@dtic.mil
WWW http://www.dtic.dla.mil/

All others may order reports through the National Technical Information Service:

NTIS
5285 PORT ROYAL RD
SPRINGFIELD VA 22161
Telephone 1 703 487 4650
1 703 487 4639 (TDD for the hearing-impaired)
E-mail orders@ntis.fedworld.gov
WWW http://www.fedworld.gov/ntis/ntishome.html

A complete list of all CRREL technical publications is available from:

USACRREL (CECRL-LP)
72 LYME RD
HANOVER NH 03755-1290
Telephone 1 603 646 4338
E-mail techpubs@crrel.usace.army.mil

For information on all aspects of the Cold Regions Research and Engineering Laboratory, visit our World Wide Web site: http://www.crrel.usace.army.mil

Special Report 98-1

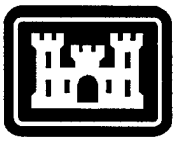

US Army Corps
of Engineers®
Cold Regions Research &
Engineering Laboratory

Quantification of Shape, Angularity, and Surface Texture of Base Course Materials

Vincent C. Janoo

January 1998

Prepared for
STATE OF VERMONT AGENCY OF TRANSPORTATION

PREFACE

This report was prepared by Dr. Vincent C. Janoo, Research Civil Engineer, Civil Engineering Research Division, Research and Engineering Directorate, U.S. Army Cold Regions Research and Engineering Laboratory. Funding was provided by the State of Vermont Agency of Transportation.

Technical review of this report was provided by Christopher Benda, P.E., State of Vermont Agency of Transportation, and by Andrew Dawson, University of Nottingham, United Kingdom. The author especially thanks Lynette Barna, Sherri Orchino, and Tim Baldwin for assistance in finding the reports and papers needed for this review, and also thanks Gioia Cattabriga for editing the report.

CONTENTS

ILLUSTRATIONS

Figure

TABLES

Table

Quantification of Shape, Angularity, and Surface Texture of Base Course Materials

VINCENT C. JANOO

INTRODUCTION

The base course layer is identified as that unbound layer between the surface course (asphalt concrete or portland cement concrete) and the subgrade. This layer is sometimes subdivided into two parts: the upper layer, called the base, and the bottom, the subbase. The base is usually constructed with coarse gravel or crushed stone, and the subbase with either gravel or sand. Several factors affect the performance of these layers. The common factors usually cited are gradation, degree of compaction, amount of fines, moisture content, and permeability. The shape, angularity, and surface texture of the aggregates also have a significant effect on the engineering response of the layer.

Quantification of the shape, angularity, and surface texture of aggregates is difficult but not impossible. There are several methods that involve either direct measurement of the aggregates or indirect inference from aggregate properties. For example, geologists have developed a sophisticated system that involves physical measurements of the aggregates, and engineers have developed visual classification methods for characterization, shape, and angularity or index tests that use some engineering properties, such as porosity, to speculate on the shape, angularity, and surface texture of aggregates. However, none of the index tests developed by engineers make it possible to quantify separately the shape, angularity, or surface texture. Usually these characteristics are lumped together as geometric irregularities.

This report reviews test methods currently available to quantify the aggregate geometric irregularities and the effect of these irregularities on the performance of base course materials. A summary of the methods used by geologists to describe aggregates has been included. Even though these methods may not be practical for everyday engineering work, they have been used by researchers for quantifying base course performance (Barksdale and Itani 1994). A review of current methods used by engineers, including a discussion on the usage of image analysis for describing particle shape and roughness, is also presented.

CHARACTERIZATION OF COARSE AGGREGATE SHAPE, ANGULARITY, AND SURFACE ROUGHNESS

The description of the aggregate particles can be conducted directly using petrological methods or by using image analysis. The effect of particle shape, angularity, and surface texture on the engineering properties can also be inferred.

Petrological methods

The shape of the aggregate can be described by its length, width, thickness, sphericity, roundness, and angularity. The surface texture is difficult to quantify and several visual charts and some sophisticated test methods have been proposed. A description of these methods is presented below.

Description of aggregate shape

Sedimentary petrologists have described the shape of particles using methods developed as long ago as 1930. The description involves mea-

surement of the aggregate dimensions (shortest, intermediate, and longest lengths). Based on these lengths, the shape of the aggregate is quantified in terms of both the flatness and elongation ratios or by the shape factor. The flatness ratio (p) is the ratio of the short length to intermediate length, and the elongation ratio (q) is the ratio of the intermediate length to the longest length.

An alternate method for describing the shape of the aggregate involves the shape factor (F) and sphericity (Ψ) of the aggregate particles. The shape factor (F) is the ratio of the elongation ratio (q) and the flatness ratio (p), i.e.,

$$F = \frac{p}{q}.$$

A shape factor equal to 1 represents a rounded or cubic aggregate. Smaller than 1, the particle tends towards being elongated and thin. Blade-shaped materials have a shape factor greater than 1.

The sphericity (Ψ) is defined as the ratio of the surface area of a sphere having the same volume as the particle in question to the surface area of the particle. The sphericity can also be determined from the flatness and elongation ratios as shown below:

$$\Psi = \frac{12.8\left(\sqrt[3]{p^2 q}\right)}{1 + p(1+q) + 6\sqrt{1 + p^2\left(1+q^2\right)}}.$$

The shape factor, p, q, and sphericity are used to classify the aggregate as disc, equidimensional, blade- or rod-shaped using Figure 1. Equidimensional can mean either cubic or round. The definitions for disc, equidimensional, blade, and rod, based on descriptions by Lees (1964) and Barksdale and Itani (1994), are presented in Table 1.

Barksdale and Itani (1994), in their study on the effect of shape, angularity, and roughness of aggregates on base course performance, used this form of shape description for characterizing the five aggregates they used. The granite gneiss, limestone, shale, quartzite, and river gravel turned out to be disc, blade, blade, blade, and equidimensional in shape, respectively. Additional discussion on the results of his study is presented later in this report.

ASTM D 2488-90 (1996), *Standard Practice for Description and Identification of Soils (Visual-Manual Procedure)*, describes the shape of aggregates as either flat or elongated, or flat and elongated using the criteria shown in Table 2. These criteria were developed basically for identifying flat and elongated aggregate and not as a general tool for describing the shape of coarse aggregates.

Description of roundness

Roundness, as opposed to shape, has to do with whether the edges are sharp or round (Wadell 1932). The roundness of a particle is sensitive to abrasion and wear to which aggregates are subjected during processing and construction. The process for determining the roundness of a particle is fairly complex and involves tracing a magnified image of the particle. An inscribed circle is drawn within the aggregate tracing and the radius of the circle is determined. The radii of

Table 1. Description of aggregate shape.

Aggregate shape	*Description*
Disc	Slabby in appearance, but not elongated
Equidimensional	Neither slabby appearance nor elongated
Blade	Slabby appearance
Rod	Elongated, but not slabby in appearance

Table 2. Criteria for describing particle shape.

Shape	*Description*
Flat	Particles with width/thickness > 3
Elongated	Particles with length/width > 3
Flat and elongated	Particles that meet criteria for both flat and elongated

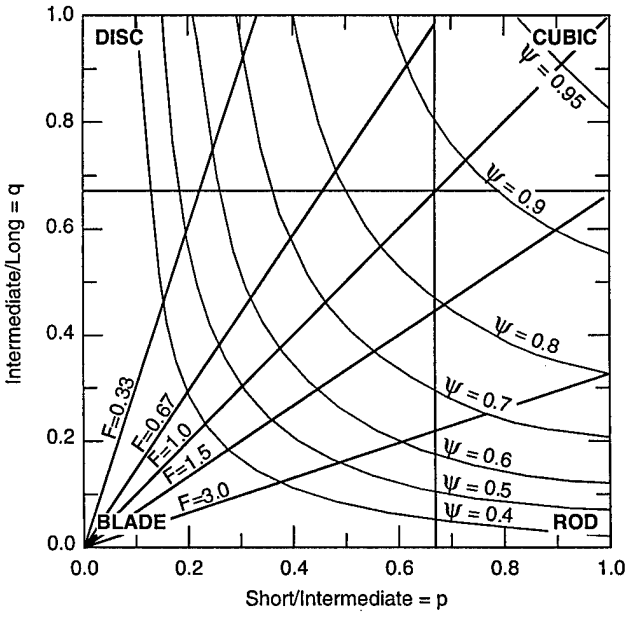

Figure 1. Aggregate classification chart.

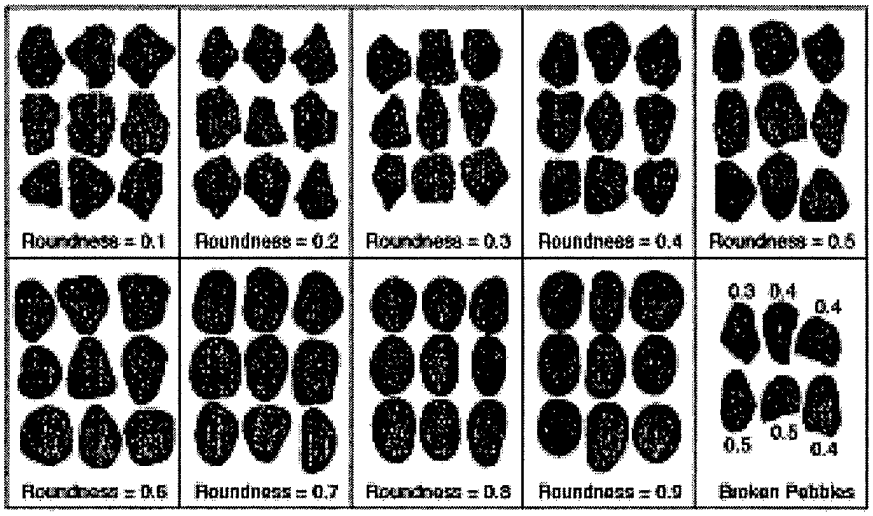

Figure 2. Roundness chart for 16- to 32-mm aggregates. (After Krumbein 1941.)

the edges and corners of the particles also are determined. These radii are used to index the roundness of the aggregate as shown below. Details on this method can be found in the papers by Wadell (1932) and Krumbein (1941). Essentially, the roundness (R) of a particle is an average measure of curvature of the corners and edges. R is expressed as

$$R = \frac{\Sigma \frac{r}{r'}}{N}$$

where r = radius of curvature of a corner of the particle surface
r' = radius of the maximum inscribed circle in the projected plane
N = number of corners.

Because this is a lengthy process, visual charts have been developed (Krumbein 1941) for estimating the roundness of aggregates. Figure 2 can be used to classify the roundness for 16- to 32-mm aggregates. By enlarging or reducing the chart, similar roundness charts could be made for other size aggregates (Krumbein 1941). The roundness (R) varies between 0.1 and 0.9. An R value greater than 0.6 indicates high roundness, R between 0.4 and 0.6 indicates medium roundness, and R less than 0.4, low roundness.

Description of angularity

Lees (1964) found that when using Krumbein's (1941) method for determining the roundness number, it was possible to get the same roundness number for two very differently shaped aggregates. He found to it to be especially true for crushed aggregates. Lees (1964) proposed a method for determining the degree of angularity, which accounts not only for the roundness of the corner but also how far the projection is from the inscribed circle (Fig. 3). The degree of angularity is calculated by the following equation:

$$A_i = (180° - a)\frac{x}{r}$$

where A_i = degree of angularity
a = measured angle
x = distance to the tip of the corner from the center of the maximum inscribed circle
r = radius of the maximum inscribed circle.

The total degree of angularity (A) is the sum of all the values for all corners measured in three mutually perpendicular planes. Again, because of the high degree of complexity, Lees (1964) developed a visual chart for determining the degree of angularity of particles (Fig. 4).

ASTM D 2488-90 (1996), *Standard Practice for Description and Identification of Soils (Visual-Manual Procedure)*, describes the angularity of coarse-grained material as either angular, subangular,

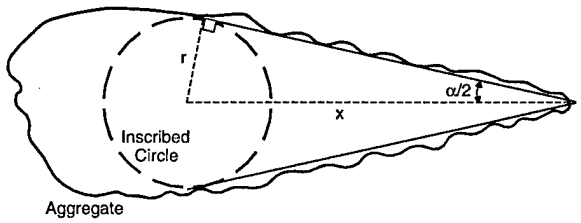

Figure 3. Parameters for determining the degree of angularity. (After Lees 1964.)

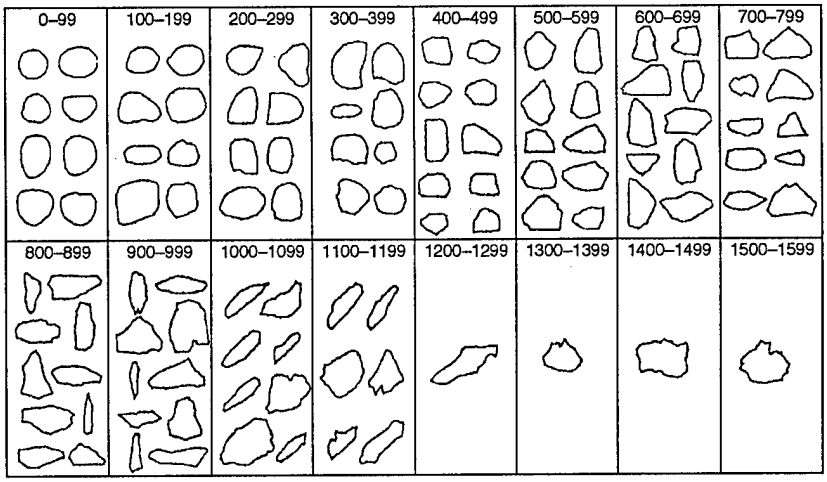

Figure 4. Degree of angularity chart. (After Lees 1964.)

Table 3. Criteria for describing angularity of coarse-grained particles (ASTM D 2488-90).

Description	*Criteria*
Angular	Particles have sharp edges and relatively plane sides with unpolished surfaces.
Subangular	Particles are similar to angular description but have rounded edges.
Subrounded	Particles have nearly plane sides but have well-rounded corners and edges.
Rounded	Particles have smoothly curved sides and no edges.

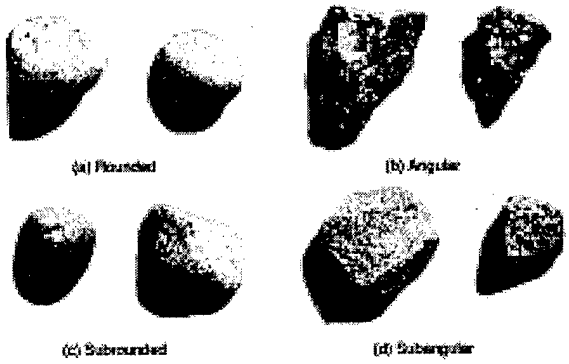

Figure 5. Visual identification of aggregate angularity. (After ASTM D 2488-90.)

subrounded, or rounded. The qualitative criteria, presented in Table 3, are used for describing the angularity. A visual chart for determining the angularity of the aggregate, similar to that found in ASTM D 2488-90, is presented in Figure 5.

Description of surface texture

The surface characteristics or texture of an aggregate are considered to have an effect on the engineering response of the material. Terzaghi and Peck (1967) defined texture as the degree of fineness and uniformity. They suggested qualitative expressions such as smooth, sharp, gritty, etc., to describe the texture.

Barksdale and Itani (1994) used a roughness scale to determine the surface texture (roughness) of aggregates. The surface roughness (*SR*) was based on visual inspection and indexed to a scale ranging from 0 (for glassy particles) to 1000 (for very rough particles).

Another method found in the literature was to coat a flat, sawed aggregate surface with asphalt (Bikerman 1964), which is then scraped to the sur-

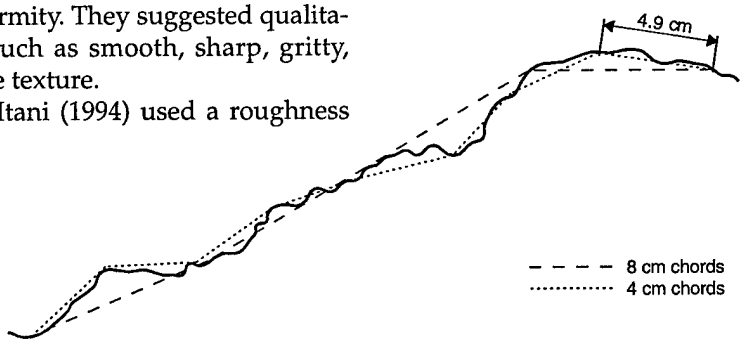

Figure 6. Measurement method for characterizing the surface texture of an aggregate. (After Wright 1955.)

face of the aggregate. The remaining asphalt on the aggregate is used as an indicator of the surface texture. This method determines the microtexture of the surface and the absorptive nature of the aggregate and is still an index to the roughness of the surface.

Wright (1955) developed a method for quantifying the surface texture of concrete aggregate particles using studies done on 19-mm stones. The test aggregates were first embedded in a synthetic resin. Once the resin hardened, the stones were cut into thin sections (approximately 2.5×10^{-2} mm thick). The thin section was placed under a projection microscope and magnified 125 times. The unevenness of the surface was traced and the total length of the trace was measured. This length was then compared with an uneven line drawn as a series of chords (Fig. 6). The difference between these two lines was defined as the roughness factor. The reproducibility of this method was reported to be good (Wright 1955). However, to obtain a reliable average of roughness of any one aggregate size, it is necessary to take many sample measurements.

Determination of aggregate characteristics using image analysis

The direct measurement methods described in the previous sections are time consuming and labor intensive. Thanks to the power of present computing capabilities, computer-based image analysis has been developed for analyzing aggregate shape, angularity, and roughness. A feasibility study was conducted for the Federal Highway Administration (FHWA) on this technology (Wilson et al. 1995). The study was conducted on fine sands (manufactured versus natural), and the conclusion was that image analysis was a viable tool for distinguishing the shape and angularity of the particles. Wilson et al. (1995) developed the Roundness and Shape Indices to quantify the roundness and angularity of the particles, respectively. The method first involves capturing images of the aggregates using a high-resolution video camera. Then an image analysis computer program is used to identify, separate, and trace the edges of the aggregates. Based on the traces, algorithms in the programs are used to determine the different characteristics of the aggregates.

The Quebec Ministry of Transportation (QMOT) uses image analysis on a routine basis for verifying the angularity of its hot mix aggregates. To study the feasibility of this method, samples of base course aggregates obtained from the Vermont Agency of Transportation (VAOT) were characterized using the QMOT image analysis system. The samples included one sample of crushed gravel and two samples of crushed stone. The crushed stone was obtained from two different sources. Roughly thirty to forty randomly selected aggregates were placed on a light table and videotaped. The outlines of aggregates from the three sources, as reproduced by the image analysis program, are shown in Figures 7 to 9.

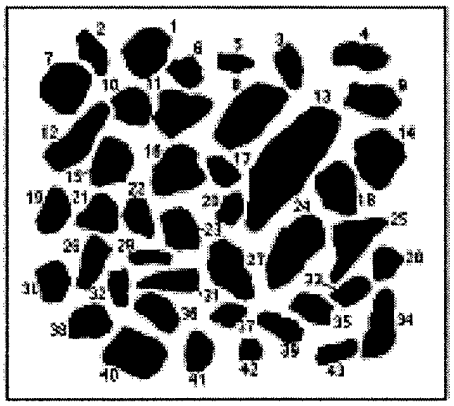

Figure 7. Image of the Pike crushed stone prior to image analysis.

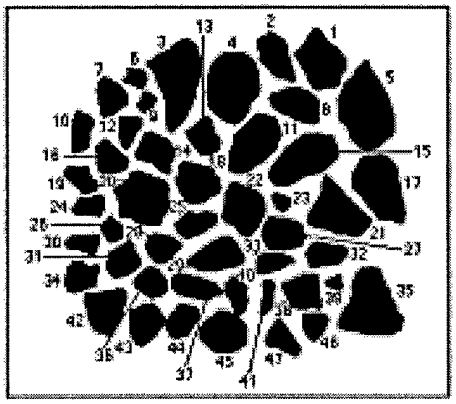

Figure 8. Image of the crushed stone prior to image analysis.

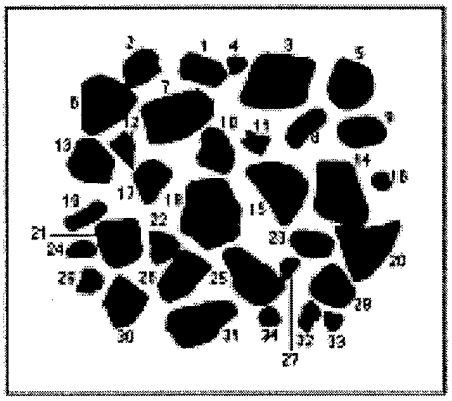

Figure 9. Image of the crushed gravel prior to image analysis.

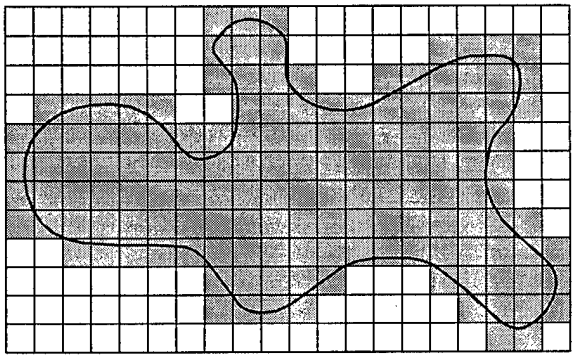

a. Area of an aggregate calculated through image analysis.

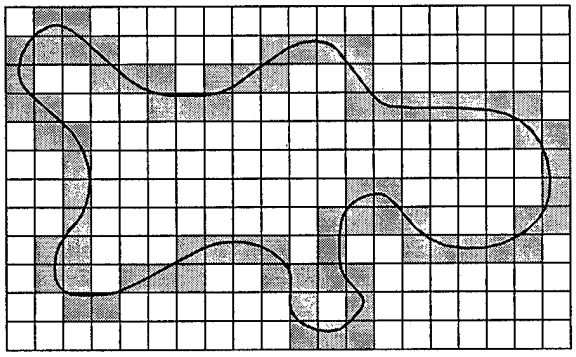

b. Perimeter of an aggregate calculated through image analysis.

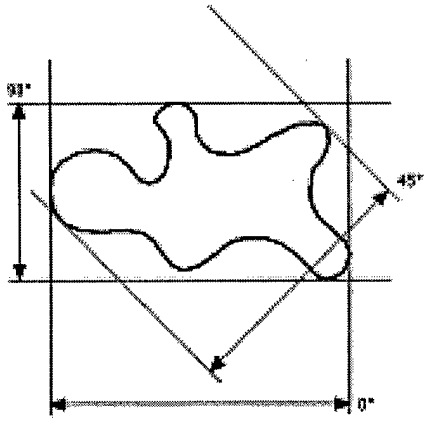

c. Typical feret measurement.

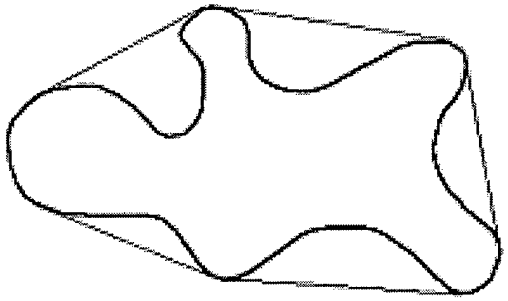

d. Illustration of convex perimeter.

Figure 10. Material characterization using image analysis.

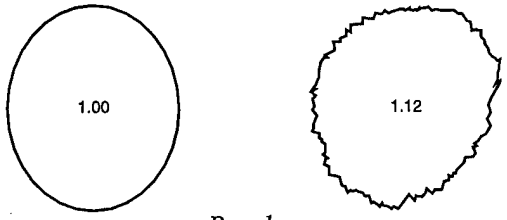

a. Roughness.

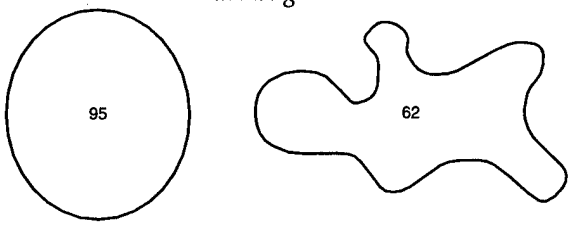

b. Roundness.

Figure 11. Definition of roughness and roundness.

The numbers on these figures are used to identify the measurements of the individual aggregates during the analysis process. The following basic measurements were made: 1) feature area, 2) feature perimeter, 3) feature ferets, and 4) x-y coordinates. In the image analysis method, the area of an aggregate is the sum of pixels present within the aggregate boundary (Fig. 10a). The perimeter is the sum of pixels surrounding the aggregate (Fig. 10b). Ferets are straight-line measurements made between two tangents (Fig. 10c). In this particular case, eight feret measurements are taken at 0, 22.5, 45, 67.5, 90, 112.5, 135, and 157.5 degrees. From these measurements, indices for roundness and roughness are derived. For example, the length and width of the aggregate are the longest and shortest feret measurements taken at the various angles mentioned above, respectively.

The roughness is defined as the ratio of the perimeter to the convex perimeter. The convex perimeter is defined as the string measurement around the tips of the eight ferets (Fig. 10d). For a smooth material, the roughness factor equals 1.00. As the roughness increases, the roughness factor also increases (Fig. 11a).

The roundness is defined as follows:

$$R_n = \frac{4\pi A}{p^2}$$

where R_n = roundness index

A = area of aggregate
P = perimeter of aggregate.

The roundness index for a perfect circle is 100. However, with image analysis, because of the square pixels matrix, the best that can be obtained is 95. As the material becomes angular, the roundness index decreases (Fig. 11b).

The results of the tests conducted on the VAOT aggregates are shown in Tables 4 to 6. The mean and variance of the roundness and roughness for the three aggregates are shown in Table 7. On the average, the results from crushed gravel as compared to the results from crushed stone indicate a decrease in roundness and an increase in roughness, suggesting that the crushed stone is more angular and rougher. The roundness index ranged from 78.54 to 72.36 for crushed gravel to crushed stone, respectively, indicating by definition that all the materials are fairly angular. The results appear to be close to one another and it is unclear at this time whether this is the range one can expect between crushed gravel and crushed stone. Visual examination of the crushed gravel and crushed stone showed that the crushed gravel mostly had one fractured face with the remainder of the body being rounded. The crushed stone had several fractured faces and was definitely more angular than the crushed gravel. Statistically, however, at the 95% confidence level, the roundness mean value between crushed gravel and crushed stone is significantly different. The mean roundness values between the crushed stones are not significantly different at the 95% confidence level.

The mean roughness values ranged from 1.031 to 1.050 for the crushed gravel and crushed stone, respectively. Again, the range is fairly small, even though the crushed gravel was fairly smooth and the crushed stone was rough. Statistically there is

Table 4. Image analysis results for crushed gravel.

	Calibration: 0.2639 mm/pixel						
Aggregate	*Length*	*Width*	*Breadth*	*Area*	*Perimeter*	*Roundness*	*Roughness*
1	19.6069	11.9607	13.9666	184.3518	55.0471	76.4519	1.0379
2	17.3974	13.5917	15.1222	171.3743	51.4075	81.4897	1.0371
3	32.8975	22.6729	24.7369	523.6398	90.942	79.5635	1.0365
4	8.8634	7.0677	8.0576	45.2048	25.7946	85.3764	1.0106
5	20.6594	18.0406	18.8365	284.5665	63.7988	87.8554	1.0327
6	24.9787	21.487	21.487	378.1483	76.026	82.2143	1.0298
7	29.8133	19.0284	23.0986	446.1356	84.5824	78.364	1.0295
8	19.8755	9.4006	9.4006	143.617	51.2797	68.6316	1.0258
9	19.2669	12.8389	12.8389	194.0849	53.7019	84.5712	1.0193
10	20.1157	14.7801	15.1222	204.8994	56.8332	79.7161	1.0421
11	11.6129	8.155	9.834	66.8338	35.615	66.2125	1.0762
12	15.4945	9.2375	10.0815	90.6258	40.2236	70.3881	1.0132
13	20.4127	17.1896	17.1896	256.1603	61.3262	85.5913	1.0288
14	30.8876	20.9589	22.83	436.9793	84.7282	76.4918	1.0432
15	27.4552	20.4127	21.2242	380.6716	80.5014	73.8164	1.0377
16	8.8634	7.7891	7.7891	47.0072	25.8876	88.1435	1.0012
17	17.4827	14.3263	15.8358	174.2582	52.825	78.4736	1.0339
18	28.7389	24.2815	27.1274	520.9001	89.8696	81.0474	1.0431
19	17.7753	7.6114	7.6114	103.7474	46.2675	60.9026	1.0454
20	29.2761	23.6358	23.6358	380.3112	85.3504	65.6051	1.0458
21	21.7556	18.5712	20.6813	296.1741	66.4352	84.3258	1.0346
22	13.9666	12.6686	13.4294	121.5554	43.8107	79.5837	1.038
23	18.4751	11.1999	11.1999	159.5504	50.0157	80.1486	1.0175
24	12.1408	7.3755	7.3755	69.6456	32.8435	81.1344	1.0132
25	28.7389	16.6525	16.6525	342.4603	76.8337	72.8982	1.042
26	23.0986	15.0409	15.0409	264.5235	66.0363	76.2269	1.0287
27	10.8734	7.1632	7.1632	50.4678	29.1575	74.5975	1.0173
28	18.2129	15.8467	17.2447	220.7607	56.0032	88.4516	1.0181
29	12.6236	9.8162	10.4749	85.3627	36.7793	79.2995	1.0404
30	21.0339	16.1835	17.9472	242.8945	61.7914	79.9413	1.0414
31	28.6527	17.1255	17.1255	352.1213	77.1649	74.3126	1.0277
32	12.8389	7.6938	8.9736	71.5922	34.6879	74.7685	1.0324
33	9.4006	7.6938	8.0576	48.5212	26.73	85.3384	1.0048
34	9.5015	8.155	8.4682	57.3891	28.5749	88.3224	1.0175

Table 5. Image analysis results for crushed stone.

Aggregate	Calibration: 0.2294 mm/pixel						
	Length	*Width*	*Breadth*	*Area*	*Perimeter*	*Roundness*	*Roughness*
1	21.2604	15.6775	15.6775	232.649	63.0996	73.4272	1.0578
2	18.9059	11.0664	11.6703	142.268	51.434	67.5796	1.0624
3	31.5722	18.8073	18.8073	355.915	85.4471	61.2578	1.0704
4	24.9255	18.578	18.578	349.272	73.4803	81.2889	1.054
5	30.3853	18.6746	20.1835	404.154	82.9949	73.7316	1.0598
6	9.5696	6.8506	8.636	48.4026	28.807	73.2963	1.0492
7	14.0057	11.2385	11.2385	110.254	43.5542	73.0368	1.0679
8	18.9059	11.3389	13.771	156.533	52.7291	70.748	1.0552
9	7.6082	6.4554	7.0868	34.3555	23.1985	80.2209	1.0199
10	15.1185	8.7156	9.4526	96.5331	42.2237	68.0413	1.0606
11	24.741	14.938	14.938	263.574	67.8068	72.0387	1.0657
12	12.9925	9.4526	9.4526	77.1502	37.4273	69.2103	1.038
13	14.4805	10.1442	12.3853	112.431	43.2809	75.4231	1.0468
14	16.7721	11.8113	13.8331	134.809	47.7635	74.2566	1.0435
15	26.1415	14.6461	15.8716	290.797	70.6654	73.179	1.0426
16	13.3041	11.4369	11.4369	105.571	40.6152	80.4227	1.0317
17	26.9299	17.0608	17.0608	315.026	74.0828	72.1309	1.053
18	17.0386	14.7553	14.938	175.317	52.3988	80.2398	1.0473
19	13.8331	8.636	9.6853	80.6892	37.422	72.4056	1.0453
20	21.7329	18.1895	19.8274	280.942	69.0353	74.0771	1.0717
21	24.0951	17.272	20.9801	272.666	72.2669	65.609	1.0694
22	19.843	15.8257	16.1386	206.896	57.8413	77.7113	1.0552
23	8.4026	6.1419	6.302	35.1722	23.407	80.6712	1.0166
24	13.6025	8.5459	9.2128	74.4279	37.2186	67.5191	1.0483
25	14.9858	9.2128	9.2128	98.1665	41.7519	70.7655	1.0577
26	10.2076	8.0693	8.4862	56.8418	29.9594	79.5815	1.0402
27	15.6382	11.6319	14.4712	141.233	46.6503	81.5526	1.0328
28	13.0734	10.6823	10.6823	96.7509	38.9508	80.1367	1.0394
29	19.7248	11.8113	13.0562	163.012	53.9461	70.3897	1.0414
30	12.6803	7.5963	9.2128	67.4588	35.3028	68.0188	1.041
31	14.4098	10.7367	11.5275	110.199	41.9611	78.649	1.0484
32	14.7553	9.258	10.394	102.359	41.7006	73.9692	1.0366
33	13.8331	7.7955	7.7955	73.5023	38.041	63.8273	1.0639
34	14.0044	11.3945	12.8373	106.551	42.4731	74.2231	1.0618
35	25.9849	21.9023	21.9023	360.488	81.5685	68.0858	1.0696
36	12.2192	10.394	10.394	93.8108	36.6085	87.9627	1.0195
37	18.2135	9.2128	9.2128	116.842	46.6123	67.578	1.042
38	15.6775	13.0562	14.1736	137.096	48.3262	73.7679	1.0604
39	7.469	5.4332	5.8352	26.2431	21.3065	72.6444	1.0299
40	14.2378	8.1692	8.1692	74.809	38.5005	63.4207	1.0791
41	12.5814	5.9633	5.9633	50.8527	33.3541	57.4416	1.0601
42	17.7389	14.9083	17.272	176.188	55.1821	72.7092	1.0477
43	15.6674	12.6803	13.0734	136.333	46.3733	79.6666	1.0464
44	13.771	10.1442	10.2699	100.617	40.2379	78.0924	1.0545
45	17.6606	14.7179	14.7179	185.988	53.6087	81.325	1.0507
46	10.8664	9.4526	10.3748	72.7945	34.5787	76.5055	1.046
47	14.6461	9.8031	11.0664	92.4496	41.7757	66.5681	1.0512

Table 6. Image analysis results for Pike crushed stone.

Aggregate	Calibration: 0.2294 mm/pixel						
	Length	*Width*	*Breadth*	*Area*	*Perimeter*	*Roundness*	*Roughness*
1	16.805	13.538	13.538	176.732	51.8708	82.543	1.0405
2	15.827	8.4026	9.4526	90.3262	41.1471	67.0417	1.0515
3	15.667	9.633	9.633	103.067	43.7545	67.6522	1.062
4	18.578	9.7328	9.7328	129.31	49.0426	67.5608	1.0528
5	11.927	6.4094	6.4094	57.1685	32.7019	67.177	1.0416
6	11.989	9.8031	9.9215	80.2537	35.675	79.2404	1.0421
7	17.983	15.216	17.008	201.342	55.3385	82.6209	1.0403
8	26.975	14.238	17.008	283.665	71.4636	69.7984	1.0422
9	18.119	11.103	11.395	142.431	50.9346	68.9905	1.0653
10	14.064	12.284	12.284	123.212	43.9718	80.0779	1.0481
11	19.366	15.119	15.119	187.023	56.9493	72.4647	1.055
12	26.375	10.97	10.97	203.629	67.5039	56.1554	1.0598
13	44.581	17.972	17.972	571.848	110.89	58.4399	1.0549
14	19.228	16.369	16.514	220.562	59.3079	78.7978	1.0622
15	16.572	12.911	14.705	157.731	50.2971	78.35	1.0454
16	19.139	15.119	15.872	199.6	56.5684	78.383	1.0454
17	12.371	8.4026	8.4026	73.2846	34.2501	78.5052	1.028
18	17.506	13.372	14.471	170.634	51.9485	79.4565	1.0432
19	15.355	9.6831	9.6831	115.753	43.3612	77.3639	1.0529
20	11.67	8.0693	8.8694	67.5677	33.2904	76.6144	1.0447
21	14.525	12.819	13.465	124.573	44.5351	78.9275	1.032
22	14.41	9.222	9.222	94.4641	39.4399	76.3141	1.0478
23	15.872	11.528	12.604	131.052	45.0253	81.2343	1.0339
24	26.694	14.238	15.216	265.262	70.3584	67.3368	1.0648
25	26.375	13.538	13.538	193.937	68.2007	52.3954	1.061
26	17.481	8.9915	8.9915	116.079	47.9728	63.3832	1.0528
27	21.24	12.45	14.004	187.894	59.0315	67.757	1.0712
28	12.137	10.144	10.27	85.6983	37.1706	77.944	1.0424
29	14.22	5.2225	5.2225	58.1485	35.2694	58.7426	1.0302
30	14.006	11.239	11.239	112.921	42.5066	78.5367	1.0516
31	19.954	8.3085	8.3085	114.283	51.2623	54.6503	1.047
32	12.819	7.1101	7.1101	68.6566	35.3577	69.012	1.0468
33	13.603	8.5042	8.5042	85.5894	36.9959	78.5818	1.0178
34	23.623	11.239	11.297	170.471	59.6085	60.2898	1.0516
35	14.471	9.6853	10.97	104.264	41.589	75.7512	1.0404
36	15.405	10.27	10.27	119.074	43.9583	77.4362	1.0388
37	11.758	8.5042	8.5042	66.3699	32.9214	76.953	1.0414
38	15.405	11.632	13.071	129.037	45.6937	77.6627	1.0459
39	15.447	8.2679	8.2679	95.7164	42.0252	68.1047	1.0519
40	20.642	13.701	16.38	218.384	59.4373	77.6804	1.0508
41	13.294	9.4037	9.4037	93.5385	38.5616	79.0477	1.0447
42	8.8694	7.5688	8.4026	45.8981	27.0922	78.5808	1.0495
43	14.471	7.323	10.27	79.9814	38.4093	68.1281	1.0337

Table 7. Mean and variance of roughness and roundness values from image analysis.

Aggregate type	Roughness		Roundness	
	Mean	Variance	Mean	Variance
Crushed gravel	1.0306	0.000211	78.537	46.668
Crushed stone	1.0500	0.000198	73.285	37.846
Pike crushed stone	1.0471	0.000115	72.365	66.589

a difference between the crushed gravel and crushed stone. There was no difference in the mean roughness values between the crushed stones. From these very limited tests on coarse aggregates, and without additional strength/modulus related testing, it is not certain whether image analysis can clearly distinguish the shape, angularity, and roughness of different aggregates.

Determination of aggregate characteristics from indirect methods

It is clear from the above discussions that the determination of aggregate shape, angularity, and surface texture is a fairly lengthy and laborious task. An alternate approach taken by engineers is to infer these characteristics from the mass properties of the aggregates. Several indices for coarse aggregates, such as angularity number, particle index, rugosity, uncompacted void, and time index have been identified in the literature.

Angularity number

The angularity number (AN) developed by Shergold (1953) is recommended by British Standards (BS 812 1975) for indexing the angularity of natural and crushed aggregates used in concrete. Shergold found that when the aggregates were compacted in a prescribed manner, the percentage of voids in the aggregate mass decreased as the aggregates became more rounded. He also found that as the amount of round gravel increased in a mixture of natural and crushed aggregates, the percentage of voids also decreased. Based on his study of six aggregates, he found that the minimum percentage of voids in rounded gravel was approximately 33%. The tests were conducted on 19-, 12.7-, 9.5-, 6.35-, and 4.76-mm aggregates. The test procedure involved compaction of individually sized aggregates in three layers in a 2800-cm^3 mold. Each layer was compacted with a tamping rod that weighed between 900 and 950 grams to 100 blows. The percentage of voids was calculated by using the net weight of the aggregate in the mold.

Using round gravel as a reference point, Shergold characterized the angularity of all other aggregates as the difference between the percentage of voids and 33%. Then, AN was found to range between 0 and 12:

$$\text{AN} = \text{percentage of voids} - 33$$

$$\text{AN} = 67 - \frac{100M}{cG_a}$$

where M = mass of standard volume of aggregate (g)
c = mass of water required to fill the same volume (g)
G_a = oven-dried specific gravity of the aggregate.

Several limitations of the angularity number were pointed out by Lees (1964). Primarily, the AN was developed based on results from only six samples of coarse aggregate. Furthermore, the angularity as described by Shergold, "angular to rounded," was based on a consensus reached from visual examination of the test aggregate by 25 observers. Another quirk with the AN was that it was not to be applicable to all shapes (such as regular geometric objects [spheres and cubes]), and the AN for perfect spheres was found to be higher than for perfect cubes, which appears to be contradictory. Furthermore, the heavy compaction required may break the aggregates, causing artificial changes in angularity.

Gupta (1985) refined the AN model to account for the shape of the aggregate. The AN was calculated in the same manner as before, with the exception that Gupta defined the percentage of voids in an aggregate mass as a function of the shape and the average size of the aggregate (mm). Based on test results of the three different aggregates, angular limestone (6- to 50-mm range), subangular crushed quartzite (6- to 50-mm range), and rounded gravel (6- to 100-mm range), as well as different proportions of limestone and rounded gravel mixtures, he found that the percentage of voids (Fig. 12) can be expressed as

$$\eta = Cd^n$$

where η = percentage of voids
C = shape factor
d = volume mean aggregate diameter (mm)
n = exponent.

The size (d) is determined by taking a known number of particles and soaking them in water

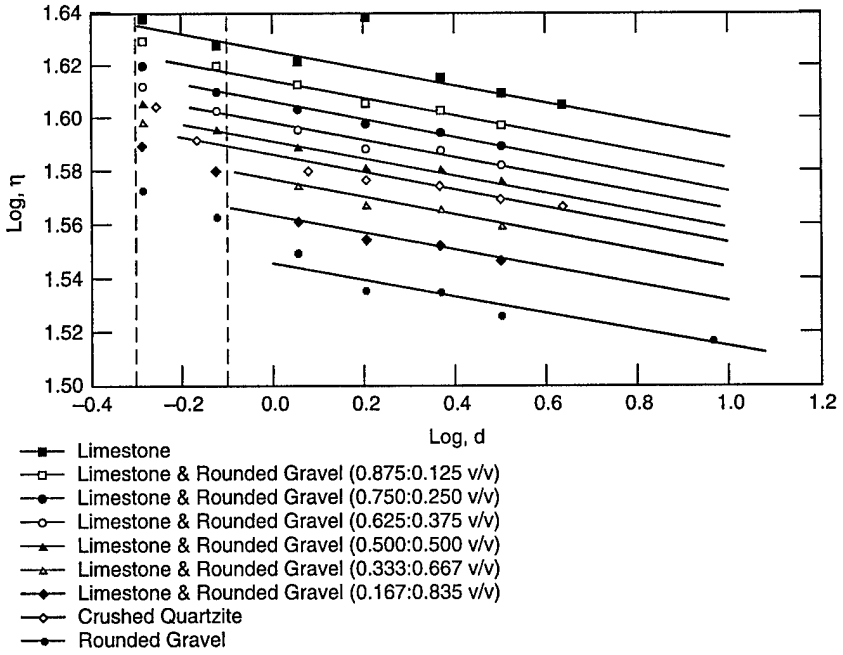

Figure 12. Relationship between mean aggregate diameter and porosity. (After Gupta 1985.)

for 24 hours. The amount of water displaced by these particles is the volume of the aggregates. Gupta (1985) divides this volume by the number of particles to get the mean volume size of the individual particles. The mean volume size is then converted to the volume mean diameter. The exponent (n) was found to be a constant equal to –0.032 for all the materials and mixtures tested.

The coefficient C was found to be a function of the aggregate shape. It was also found to be a function of the amount of rounded gravel in the mixture. Values of C as reported by Gupta (1985) are presented in Table 8. The coefficient C ranged between 39 and 45 and was found to decrease as the material changes from an angular to a rounded material. Also, C decreased as the amount of rounded gravel in a mix increased.

Gupta (1985) also reported that the size of similarly shaped material had an effect on the percentage of voids. For all of the materials tested, he found that the percentage of voids decreased as the size of aggregate increased. For example, he reported a 5% decrease in porosity when the mean size of rounded gravel increased from 5 mm to 32 mm. Likewise, a 3% decrease in porosity was reported for a similar change in aggregate size for angular limestone. Therefore, the size of the particles has an effect on the AN value. When using AN to characterize angularity it is important to ensure that the comparison is done on material of the same size.

Table 8. Value of shape factor (C) for various materials. (After Gupta 1985.)

Materials	*Value of* C
Angular limestone	45.43
Subangular crushed quartzite	41.44
Rounded gravel	37.89
Limestone + rounded gravel (0.875 : 0.125 v/v)	43.49
Limestone + rounded gravel (0. 75 : 0.25 v/v)	42.63
Limestone + rounded gravel (0.50 : 0.50 v/v)	41.98
Limestone + rounded gravel (0.333 : 0.667v/v)	40.58
Limestone + rounded gravel (0.167 : 0.733v/v)	39.40

Particle index

The particle index (I_a) is based on the concept that the shape, angularity, and surface texture of a uniformly (single) sized aggregate affects not only the void ratio but also the rate at which the voids change when the aggregate is compacted in a standard mold (Huang 1962). Through experimentation with different types of molds and different types of aggregates, and with a specific procedure, Huang (1962) found a linear relationship between the number of compactive strokes (10 to 50) and the void ratio. There was no general relationship found with fewer than 10 compactive strokes. The resulting change in the void ratio became insignificant when more than 50 compactive strokes were used (Huang 1962). The hypothetical void ratio at zero strokes was linearly extrapolated from the measured void ratio at the end of 50 strokes and the rate of void change

between 10 and 50 strokes. It was found to be dependent on the shape, angularity, and texture of the aggregates. Huang (1962) found that this "zero stroke void ratio" became smaller as the aggregate became more spherical, rounded, and smooth. He also found that this was more pronounced when the mold was rhombohedron shaped.

The particle index test initially was developed for three aggregate sizes: passing the 19-mm and retained on the 12.7-mm sieve, passing the 12.7-mm and retained on the 9.5-mm sieve, and passing the 9.5-mm and retained on the No. 4 (4.75-mm) sieve. For each size, the test involves tamping the uniform-sized aggregate into a mold in three equal layers using a standard tamping rod with 10 strokes per layer. The tamping rod is raised to a height of 50 mm from the top of the aggregate surface. At the end of the third layer, material is added to make sure that the aggregate surface is flush with the rim of the molds. The test is repeated using 50 strokes. The percentage of voids in the aggregate is calculated using the following equation:

$$V_n = \left[1 - \frac{W_n}{S * v}\right] \cdot 100$$

where V_n = percentage of voids at n strokes per layer
W_n = net weight of aggregate in the mold at n strokes per layer (g)
s = bulk density of the aggregate (g/cc)
v = volume of mold (cc).

The particle index (I_a) is calculated using the formula

$$I_a = 1.25V_{10} - 0.25V_{50} - 32$$

where V_{10} = percentage of voids in aggregates at 10 strokes per layer
V_{50} = percentage of voids in aggregates at 50 strokes per layer.

Typical particle index results reported by Huang (1962) are shown in Table 9. Sizes 1, 2, and 3 represent aggregates passing the 19-mm and retained on the 12.7-mm sieve; passing the 12.7-mm and retained on the 9.5-mm sieve; passing the 9.5-mm and retained on the No. 4 (4.75-mm) sieve, respectively. Shapes, a, b, and c represent bulky, elongated, and flat particles, respectively. Gravel (ii) was visually classified as gravel with smooth surfaces and rounded corners. Gravel (iii) was classified as gravel with rough surfaces and sharp corners and edges. Crushed gravel (p) was made up of gravel aggregates as received from the plant. No screening between crushed and uncrushed gravel was made. Crushed gravel (pp) was made up of those that were sorted to have at least one crushed face. The shapes, angularity, and roughness classifications were based on visual observations by several operators and were not based on any measurements (Huang 1962). The results indicated that the test method is capable of distinguishing the difference between smooth, rounded and rough, angular aggregates by the increasing particle index from gravel to crushed stone. It also appears that this index is capable of distinguishing different levels of crushed gravel. A modified version of this test has been standardized by ASTM. The test is designated as ASTM D 3398-93 (1996), *Standard Test Method for Index of Aggregate Particle Shape and Texture* (1996), and it covers both coarse and fine aggregates. For the coarse portion, the maximum size has been increased to 38 mm. Depending on the size of the aggregates, different size molds are used, as shown in Table 10. The mold as prescribed by this standard is cylindrical in shape. Although the effect of this test method was more pronounced in a rhombohedron-shaped mold, it could also be seen to a lesser degree with a circular mold.

The problem with this test method, with respect to coarse aggregates, is in the determination of the volume of voids. Initially, the voids were calculated based on the volume of the mold. This required making certain that the aggregates were filled to the rim of the mold and the aggregates' surfaces were flush with the rim. Because of this it was found that the results were operator dependent.

Table 9. Results of particle index tests for various aggregates. (After Huang 1962.)

	Size 1			*Size 2*			*Size 3*		
Sample	*Shape a*	*Shape b*	*Shape c*	*Shape a*	*Shape b*	*Shape c*	*Shape a*	*Shape b*	*Shape c*
Gravel (ii)	7.5	8.7	9.8	7.1	9.1	9.4	7.5	8.5	—
Gravel (iii)	8.8	10.0	13.2	9.0	10.2	14.0	9.1	10.4	12.2
Crushed gravel (p)	9.5	11.7	13.6	—	—	—	—	—	—
Crushed gravel (pp)	11.3	14.6	14.8	—	—	—	—	—	—
Crushed stone	13.4	16.0	16.9	12.4	15.9	17.4	12.6	14.9	16.4

Table 10. Mold size and dimensions of tamping rods for the particle index test. (After ASTM D 3398-93.)

Aggregate size (mm)		Mold/Rod	Aggregate specimen size	Mold diameter	Mold height	Rod diameter	Rod length	Mass of rod
Passing	Retained	designation	(kg)	(mm)	(mm)	(mm)	(mm)	(g)
38.1	25.4	A	13.6	203.2 ± 0.2	237.0 ± 0.2	21.2 ± 0.2	814 ± 0.2	2204 ± 10
25.4	19.0	B	13.0	152.4 ± 0.2	177.8 ± 0.2	15.9 ± 0.2	610 ± 0.2	930 ± 10
19.0	12.7	B	13.0	152.4 ± 0.2	177.8 ± 0.2	15.9 ± 0.2	610 ± 0.2	930 ± 10
12.7	9.5	C	4.0	101.6 ± 0.2	118.5 ± 0.2	10.6 ± 0.2	406.9 ± 0.2	276 ± 3
9.5	4.75	C	4.0	101.6 ± 0.2	118.5 ± 0.2	10.6 ± 0.2	406.9 ± 0.2	276 ± 3

Huang (1965) modified the test method to measure the actual volume of the compacted aggregate mass. This involved a special device called a volumeter, which fitted exactly over the mold. The volumeter was made up of a bottom thin flexible membrane and a standpipe. The procedure for compacting the sample remained the same, except that at the end of the last layer, a flexible membrane was placed on top of the surface and water was poured through the standpipe to a prescribed height. The idea here is that when water is introduced on top of the membrane, the thin membrane will deform to match the surface. Knowing the volume of the mold and the volume of water in the volumeter, the actual volume of the aggregate mass is calculated. Using this method for volume measurement, more reproducible results were obtained (Huang 1965). In addition to modifying the method for measuring the volume of the compacted aggregates, Huang modified the test to determine particle index of fine aggregates (passing #4 and retained on the #200 sieve).

Bindra and Al-Sanad (1983) modified the particle index test to test coarse aggregates up to 50-mm maximum size in their study. In this case, coarse aggregates are designated as any material larger than 2.36 mm (#8 sieve). The test method is similar to the procedure developed by Huang (1965) with several exceptions. The mold used is cylindrical in shape and the dimensions and weight of the mold and tamping rod sizes are different. Details on the dimensions and weights of the mold and tamping rods are shown in Table 11.

Bindra and Al-Sanad (1983) conducted tests on aggregates that ranged from natural aggregates to blast furnace slags. They also looked at the effect of different gradations (open graded to dense graded) and concluded from their study that gradation did not affect the weighted particle index value. It should be noted that the gradation study included both the coarse and fine fractions. The weighted particle index for a given gradation is the weighted mean of the percent retained in each sieve multiplied by the particle index for that size. The procedure for determining the weighted particle index is presented in ASTM D 3398 (1996). Bindra and Al-Sanad (1983) also concluded from their study that the particle index for smooth-surfaced, rounded aggregates averaged around 6.5, and for crushed, high angularity, rough-textured aggregates, the average was around 17.5.

They also proposed a new method for calculating the volume of the aggregate mass in the mold. Instead of using the volumeter device developed by Huang (1965), they proposed a sand replacement technique. This method involves placement of a thin flexible membrane on top of the aggregate surface. Sand (passing the #25 and retained on the #50 sieve) is then poured onto the surface of the membrane to the top of the mold. The net weight of sand required to fill to the rim of the mold is obtained and the volume to fill the mold is obtained. The volume of the compacted aggregate mass is the difference between the volume of the mold and the volume of sand required to fill the mold. This method appears to be easier and less cumbersome than the volumeter method.

Table 11. Dimensions of mold and tamping rods. (After Bindra and Al-Sanad 1983.)

Aggregate size (mm)	Inside diameter of mold (mm)	Inside height of mold (mm)	Diameter of tamping rod (mm)	Length of tamping rod (mm)	Weight of tamping rod (g)
20–50	250.0	291.6	26.00	1045	4120
2.36–20	152.4	177.8	15.88	610	930

Specific rugosity index

Tons and Goetz (1968) developed the packing volume concept to characterize the shape, angularity, and roughness of the aggregates used in bituminous mixtures. The test was developed for both the coarse (12.7-mm max) and fine fractions. They decided that the shape of the particle could possibly be quantified as a separate value; however, it was difficult to separate the interaction of angularity and roughness on aggregate performance. They proposed that the effect of both angularity and roughness be combined and considered in one term, "rugosity."

The assumption is that the volume of an individual particle in an aggregate mass determines the density and voids in the bulk. This volume, called the "packing volume," had to account for the volume of the solid particle, the volume of internal voids, and the volume of "outside voids." The "outside voids" volume is made up of the volume of the dips and valleys on the aggregate surface (Fig. 13). The packing volume can be imagined as a membrane around the aggregate.

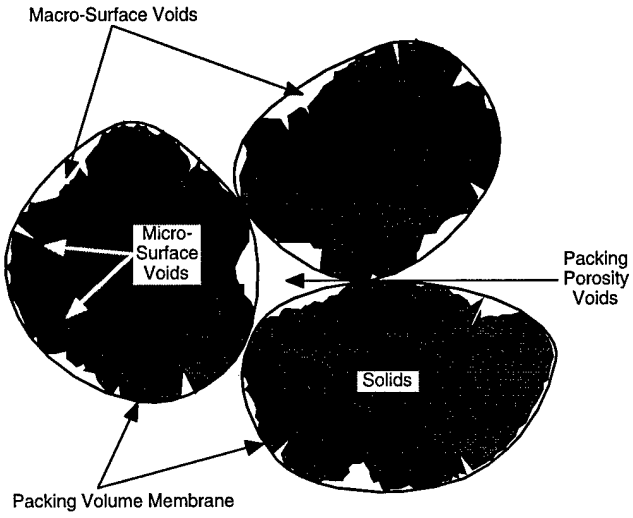

Figure 13. Packing volume, packing porosity, and geometric irregularity of aggregate particles. (After Ishai and Tons 1977.)

The packing volume membrane divides the voids into two components, the interparticle voids and particle surface voids (Ishai and Tons 1977) (Fig. 13). For one-sized particles, it is assumed that the interparticle voids are constant and this porosity is the same as that obtained from same one-sized smooth spherical particles. Tons and Goetz (1968) assumed that aggregate shape can be mathematically defined as ellipsoids. They found that the porosity calculated from ellipsoids or spheres of the same size had the same amount of voids. Any difference, then, between the porosity of the smooth spherical particles and the aggregates is due to the irregularities of the aggregates.

Ishai and Tons (1971) developed a specific rugosity (S_{rv}) index to express the total geometric irregularity of the particle. S_{rv} will be approximately equal to zero for smooth, spherical particles:

$$S_{rv} = 100\left(\frac{V_{sr}}{V_p}\right) = 100\left[1-\left(\frac{G_{px}}{G_{ap}}\right)\right]$$

where S_{rv} = specific rugosity (%)
V_{sr} = volume between the packing volume membrane and the volume of macro and micro surface voids
V_p = packing volume of the particle
G_{px} = packing specific gravity
G_{ap} = apparent specific gravity.

The apparent specific gravity of the aggregates can be calculated using ASTM Test for Specific Gravity and Absorption of Coarse Aggregate (C 127). G_{px} is determined from the pouring test developed by Ishai and Tons (1977). The test involves taking two one-sized particles and pouring them into a standard container using a standard procedure. One of the particles is used as a standard (smooth, spherical glass beads) with a known packing specific gravity, G_{ps}. The other is the test particle for which G_{px} is sought. G_{px} is a function of the ratio of the weight of the test particle to the standard particle:

$$G_{px} = \left(\frac{\Sigma W_x}{\Sigma W_s}\right) G_{ps}$$

where W_s = weight of the standard
W_x = weight of the test material
G_{ps} = packing specific gravity of standard material
G_{px} = packing specific gravity of test material.

A schematic of the pouring test is given in Figure 14. The specifications for the pouring test apparatus for the coarse aggregate fraction are given in Table 12.

Some typical results as presented by Ishai and Tons (1977) are shown in Figure 15. The specific rugosity of two sizes, 12.7 to 15.9 mm and #3 to #4 sizes for natural gravel, crushed gravel, limestone, and beach pebbles are plotted. The specific rugosity increases as the material becomes more

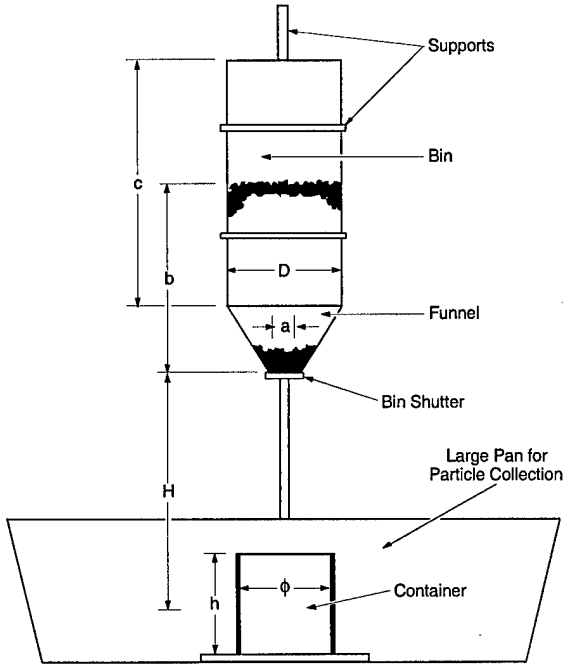

Figure 14. Schematic description of the pouring device. (After Ishai and Tons 1977.)

angular and rougher. Also shown in the figure is the effect of aggregate size on the specific rugosity. The value of the specific rugosity increases as the size of the material decreases.

Uncompacted voids in aggregates

This test method is similar to the specific rugosity test. Initially developed for fine aggregates by the National Aggregate Association, it involves allowing the fine aggregates to freely fall into a calibrated cylinder from a specified height. The exception here is that the aggregates are not separated into various sieve sizes, as is done with the other index tests. The test for fine aggregates is designated by ASTM as Test Method C 1252. The weight of aggregate and the bulk specific gravity are used to calculate the uncompacted void content:

Table 12. Specific setups for coarse fractions for the pouring test. (After Ishai and Tons 1977.)

Dimensions (cm)	*Coarse fractions*	
	12.7 to 15.9 mm	*#3 to #4*
Bin diameter	16.0	16.0
Funnel orifice diameter	3.0	1.44
Aggregate head	12.0	12.0
Pouring height	21.0	21.0
Container diameter	12.2	10.3
Container height	15.2	11.8
Bead diameter (avg.)	16.0	6.0

$$UVC = \frac{V_{cyl} - \left(\frac{M}{G_{sb}}\right)}{V_{cyl}} \times 100$$

where UCV = uncompacted void content (%)
V_{cyl} = volume of cylinder (cm^3)
M = mass of aggregate in cylinder (g)
G_{sb} = bulk specific gravity of aggregates.

UCV increases with increasing angularity and roughness of the aggregates. Aldrich (1996) modified this test for coarse aggregates. A schematic of his test apparatus is shown in Figure 16. The coarse aggregate for the test passed the 19-mm sieve and was retained on the #4 sieve. The test

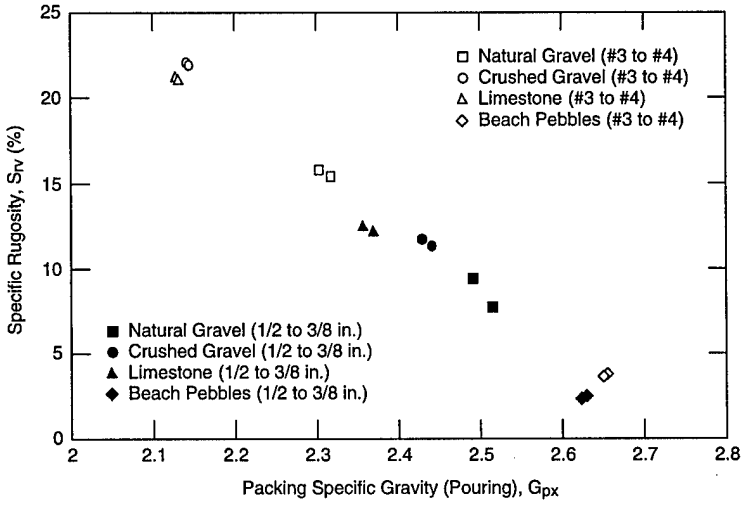

Figure 15. Packing specific gravity and rugosity for different aggregates.

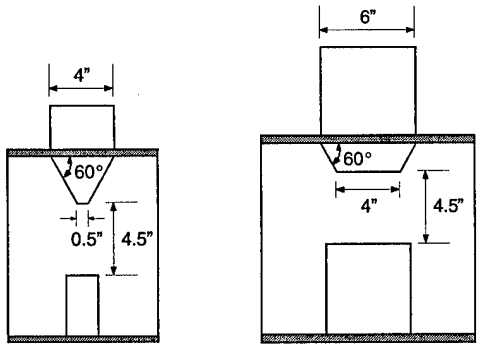

Figure 16. Test apparatus for ASTM C 1252 and modified ASTM C 1252. (After Aldrich 1996.)

apparatus, as pointed out by Aldrich (1996), is similar to that developed by Ishai and Tons (1977) for the Specific Rugosity Tests. The test method is similar to that used for fine aggregates and the uncompacted void content is calculated using the same equation used for the fine aggregates. Aldrich (1996) reported that the *UCV* increased with increasing angularity of the aggregates.

Time index

Several test methods exist for fine aggregates where the rate of flow through a standardized orifice is used to index the material shape, angularity, and texture (Rex and Peck 1956, Tobin 1978). The time of flow is usually compared to a standard material, such as Ottawa sand. A similar test method for coarse aggregates was developed by the French in 1981. The basis of this test is that the flow rate of an aggregate mass is affected by angularity, surface texture, and the bulk specific gravity of the aggregate. The equipment necessary for this type of test method can be found in the Quebec Ministry of Transportation Aggregates Laboratory in Quebec City, Quebec. Figure 17 shows the test apparatus.

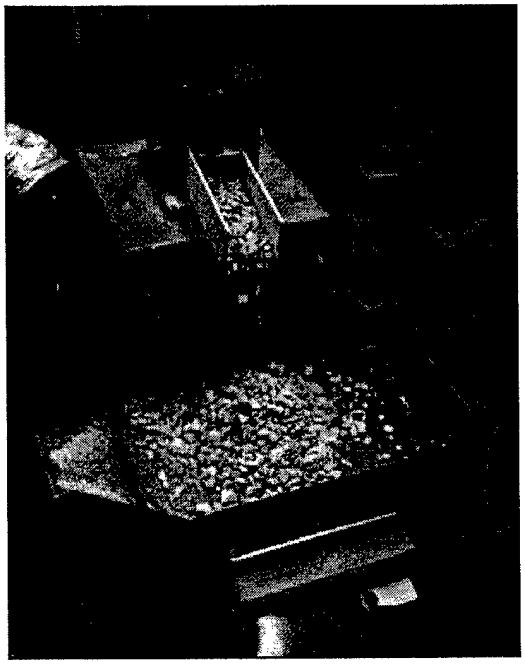

Figure 17. QMOT time index test apparatus.

The flow coefficient (C_e) of an aggregate is the time required in seconds for 7 kg of material to flow through a specified opening under a vibratory frequency of 50 Hz. The opening is 60 mm for material passing the 20-mm sieve and retained on the 4-mm sieve. The maximum size currently tested with this equipment is 20 mm. The flow coefficient (C_e) is determined from the following equation:

$$C_e = \frac{t \times G_{sb}}{k}$$

where C_e = flow coefficient
t = time (sec)
G_{sb} = bulk specific gravity
k = constant (1 second).

The test involves first drying 10 kg of aggregate. This amount is then placed into the sample tube. The vibrating table is turned on and 1 kg of material is allowed to collect in the pan on the floor. The pan is set on a scale and the weight of the aggregate in the pan is monitored. After 1 kg of material has collected in the pan, a stopwatch is turned on. The watch is stopped when an additional 7 kg of material has collected in the pan. The amount of time for 7 kg to collect in the pan is noted. The test is repeated five times and the average time value is determined.

The same material used for the image analysis was tested using this equipment. The results are shown in Table 13. The bulk specific gravity of the aggregates was assumed to be 2.6.

The results indicate that, based on the flow coefficients, crushed stone is more angular than crushed gravel. This test can be conducted quickly; further work in this area is warranted.

Table 13. Average flow coefficients for Vermont subbase materials.

Material	*Average time (s)*	*Flow coefficient*
Crushed gravel	33.45	92.2
Crushed stone	44.13	114.7
Pike crushed stone	44.62	116.0

LABORATORY RESPONSE OF ANGULAR MATERIAL

From static triaxial tests, it has been shown that rounded aggregate materials produce significantly higher permanent deformation than angular aggregate soils. This is reflected in the angle of internal friction (ϕ). During compression, it is commonly found that rounded particles are able to slip easily, whereas angular materials have to overcome the higher frictional forces at the contact interfaces. Generally, ϕ increases with increasing angularity (Holtz and Kovacs 1981). Holtz and Kovacs (1981) also found that as the surface roughness increased, so did ϕ. The effects on ϕ by angularity, surface roughness, and other factors are shown in Table 14.

Table 14. Summary of factors affecting ϕ. (After Holtz and Kovacs 1981.)

Factors	*Effect*
Void ratio (e)	$e\uparrow\phi\downarrow$
Angularity (A)	$A\uparrow\phi\uparrow$
Grain size distribution	$C_u\uparrow\phi\uparrow$
Surface roughness (R)	$R\uparrow\phi\uparrow$
Moisture content (w)	$w\uparrow\phi\downarrow$ slightly
Particle size (S)	No effect (with constant e)
Intermediate principal stress	$\phi_{ps} \geq \phi_{tx}$
Overconsolidation or prestress	Little effect

The information in Table 14 relates to static loading conditions. However, the loading condition on a pavement structure is not static, but cyclic. Also, the load levels applied are usually not near the shear strength of the material except when the material is saturated, as is the case during spring thaw. The data in Table 14 may or may not apply to pavement structures. Very little data are published on the performance of base course materials under cyclic loading. This is probably due to the erroneous assumption that failure of base course materials does not occur.

With the advent of mechanistic pavement design procedures, several studies have been presented on the resilient modulus of base materials. Base materials have been identified as stress dependent and several models exist for predicting the resilient modulus of base materials, such as the K_1–K_6 model in SUPERPAVE (Lytton et. al 1993) and the "universal" K_1–K_3 model (Witczak and Uzan 1988). However, the resilient moduli reported in the literature for natural gravel and crushed rock were quite similar to one another (Thompson and Smith 1990). They reported the range to be about 200 to 240 MPa under a bulk stress of 138 kPa. Ishai and Gelber (1982) also found similar trends for bituminous mixes. They suggested that this was to be expected because in the resilient modulus test, the applied stress levels are very low and only with near-failure conditions will the effect of the geometric irregularities be evident; for example, in terms of particle interlocking. However, the deformation under the same applied stress level, when the base course is saturated, will be high, and the angularity and roughness of the aggregates will have a greater effect on pavement performance.

There is very little information in the literature on the performance of base course layers as a function of the shape, angularity, and roughness of the aggregates. The results of only two studies on the effect of aggregate geometry and surface roughness were found in the literature. One was by Holubec and Wilson (1970) and the other by Barksdale and Itani (1994). Holubec and Wilson (1970) used crushed gravel and crushed stone in their study. They looked at the effects of angularity and the proportion of crushed material on base course performance. The samples were compacted at an optimum moisture content of 4.5% using a 4.5-kg hammer dropped 457 mm and applying 25 blows per layer. The test samples were 102 mm in diameter and 203 mm in height. The maximum aggregate size was 9.5 mm.

Holubec and Wilson (1970) report in terms of the cyclic creep strain. The definition of cyclic creep strain is unclear in the report and is taken by this author to refer to the total strain minus the elastic strain. They found that the cyclic creep strain after 5000 load repetitions decreased as the percent of crushed particles increased (Fig. 18). The samples were made by blending different amounts of crushed aggregate with the parent rounded gravel aggregates. With respect to sphericity and angularity, they reported that, as the aggregates became angular, the cyclic creep strain, after 5000 load repetitions, increased (Fig. 19). The results appeared to be contradictory, as one would expect the creep strains to decrease with increasing angularity. The results may be explained by the fact that there is a larger contact area with rounded material than with angular material. Thus it will require a larger shear force at the points of contact to move the aggregates. This could also explain why the resilient modulus reported in the literature for rounded and angular materials are similar. This is only speculation and

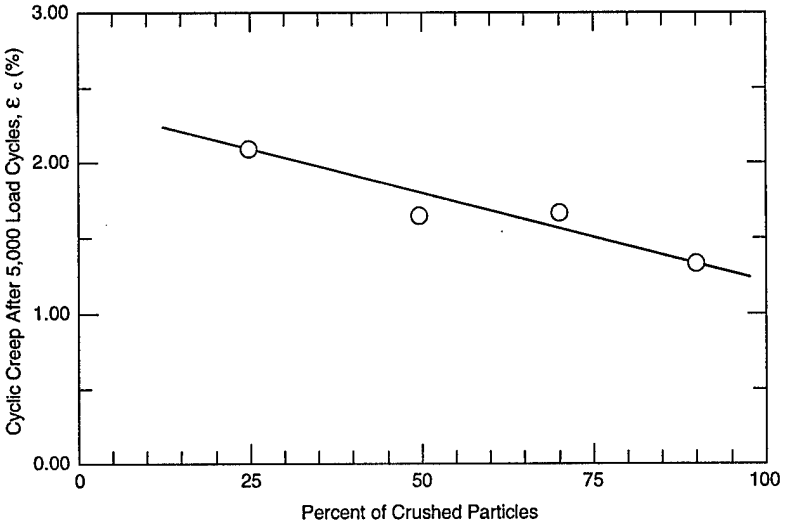

Figure 18. Effect of crushed particles on cyclic creep strain. (After Holubec and Wilson 1970.)

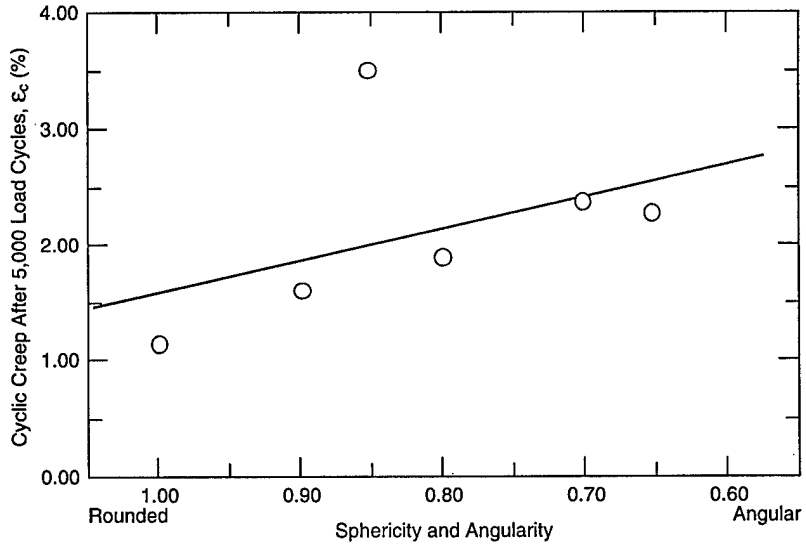

Figure 19. Effect of combined sphericity and angularity on cyclic creep of base course materials. (After Holubec and Wilson 1970.)

further work in this area may be required. In the same study, the friction angle was found to increase with increasing angularity (Fig. 20). Based on their study, Holubec and Wilson recommended that repeated load tests be conducted on characterizing the performance of base course materials and cautioned on the use of the angle of internal friction as a parameter for predicting base course performance. In my opinion, with thawing soils, the friction angle may be a good indication of the ability of the base course to resist permanent deformation. When the base is saturated, the load levels commonly applied on pavement structures when they are dry may be high enough to move the base response from the elastic to the plastic (failure) zone.

The other work was done by Barksdale and Itani (1994). They presented results of the effect of aggregate shape on the resilient and permanent deformation behavior of five base course materials. The gradation used in the study is shown in Table 15. The medium gradation in Table 15 is similar to the VAOT fine gradation for subbase of crushed gravel.

Table 15. Gradation of test aggregates. (After Barksdale and Itani 1994.)

	Percent passing					
Gradation	*38.1 mm*	*19 mm*	*9.5 mm*	*No. 4*	*No. 40*	*No. 200*
Medium	100	80	60	45	13	4
Coarse	100	65	43	27	7	0
Fine	100	85	70	58	25	10

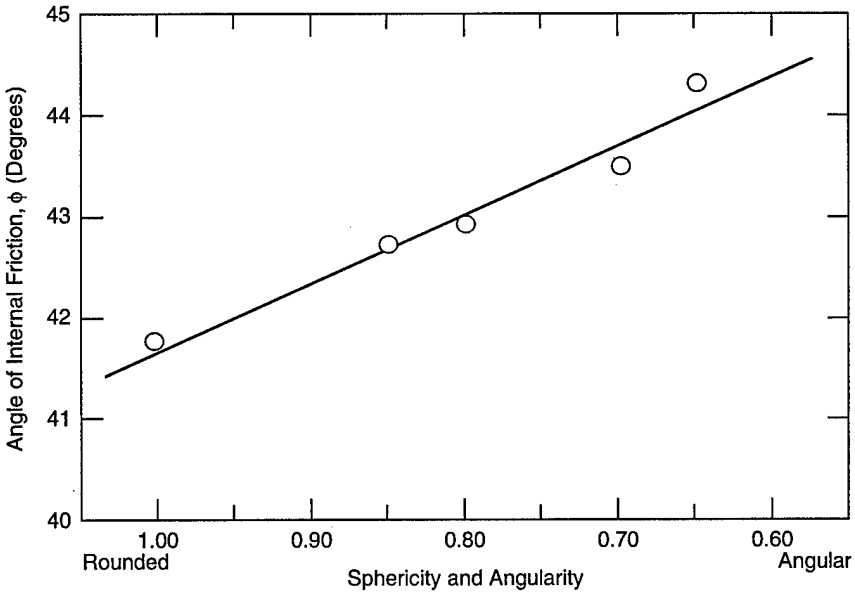

Figure 20. Effect of sphericity and angularity on the angle of internal friction. (After Holubec and Wilson 1970.)

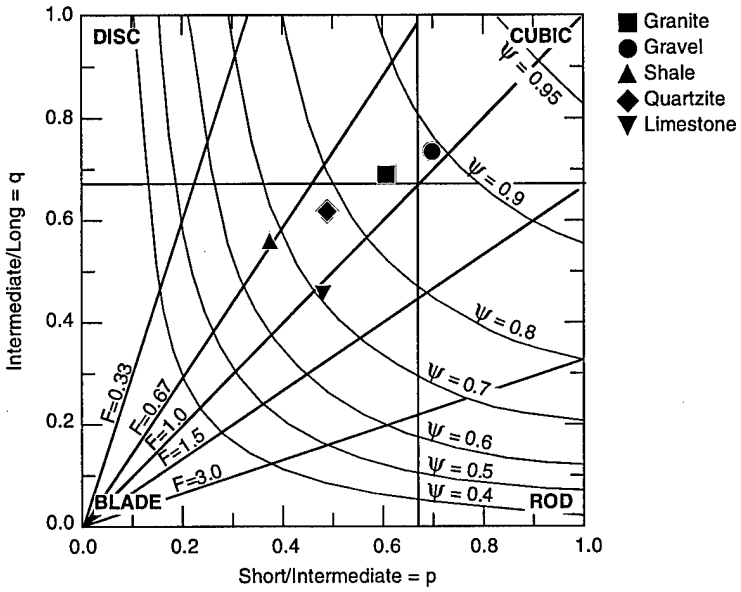

Figure 21. Shape classification of aggregates. (After Barksdale and Itani 1994.)

The test materials, shape, and surface characteristics as reported by Barksdale and Itani (1994) are shown in Figure 21. The samples were compacted using a vibratory compactor at the optimum moisture content. The test specimens were 152 mm in diameter and 305 mm in height. These dimensions are acceptable provided the maximum size of the aggregates is no more than 25 mm. Sweere (1990) found that testing aggregates containing 51-mm particles in a 152-mm-diameter mold produced inconsistent results. He recommended that, for large particle sizes, the specimen diameter be at least six to seven times the maximum particle size, to minimize the boundary effects by the large aggregates. Scalping of large aggregates and replacing equivalent amounts of smaller aggregates changes the overall structure of the material. Dawson* reported that in unreported experiments at the University of Nottingham, similar results were obtained on dry specimens in which the grading curve was

* Personal communication, Andrew Dawson, University of Nottingham, United Kingdom, 1992.

either translated laterally or truncated. This in turn produces resilient and plastic responses that may not be representative of the actual material. If there is a sufficient amount of large aggregates (greater than 10%), large-scale triaxial testing is recommended. Besides aggregate geometry, Barksdale and Itani (1994) looked at the influence of the fines, the plasticity of the fines, gradation, and moisture content on base course performance.

To quantify the effect of the aggregate geometry and surface roughness, Barksdale and Itani (1994) developed the aggregate influence factor (AIF), which was based on a multiple regression between observed laboratory performance and various indices that described the aggregate shape and texture. For the aggregates tested, they found that the AIF was a function of the sphericity, roundness, surface roughness, and angularity of the aggregate. They employed methods used by geologists to quantify sphericity and roundness as described earlier in this report. For surface roughness, Barksdale and Itani (1994) used a scale from 0 to 1000 to quantify glassy to very rough particles, respectively. They then rated the roughness of the aggregates based on visual examination. For example, for the aggregates in the study, the AIF was as follows:

$$AIF = 2500^{*} (\psi + R) - (A + SR)$$

where AIF = aggregate angularity factor
ψ = average sphericity value
R = average roundness value
SR = surface roughness coefficient.

Table 16. AIF values of test aggregates.

Base material	*AIF*
Granite gneiss	500
Limestone	50
Shale	1675
Quartzite	150
River gravel	3700

This AIF value is specific to the aggregates tested by Barksdale and Itani (1994) and is not recommended for other aggregates. If this approach is taken to characterize base course performance, new AIF values will have to be developed for other aggregates. The AIF values for the test aggregates are presented in Table 16. The AIF values decrease with increasing angularity and roughness.

The resilient modulus test was conducted using the procedure prescribed in AASHTO T-274-82. For permanent deformation studies, the specimens were subjected to 41 kPa confining pressure and subjected to 70,000 load repetitions at a principal stress ratio of four or six. Barksdale found the resilient modulus of rough angular materials to be higher than the rounded material by about 50% at low bulk stress values and about 25% at high bulk stress values (Fig. 22). This is much higher than the values reported by Thompson and Smith (1990). There appears to be some inconsistency in the results found in the literature. The effect of moisture was also pronounced. Barksdale and Itani (1994) reported that under drained conditions, the resilient modulus

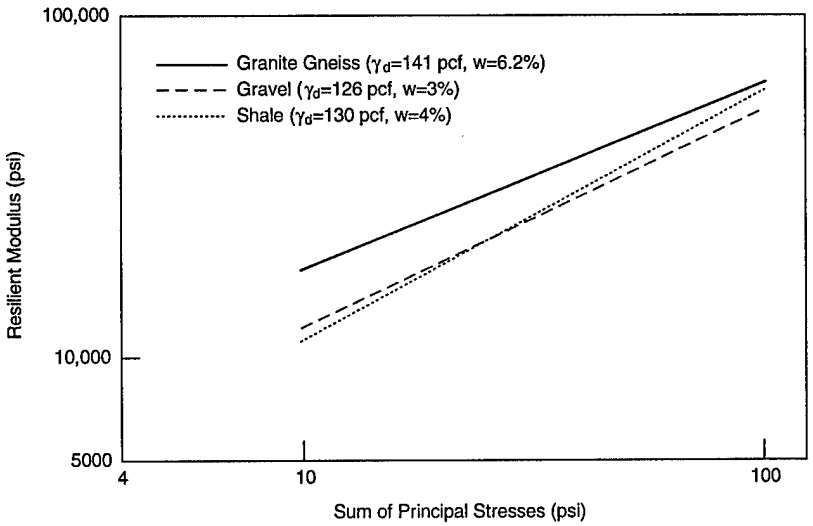

Figure 22. Influence of material type and state of stress on resilient modulus. (After Barksdale and Itani 1994.)

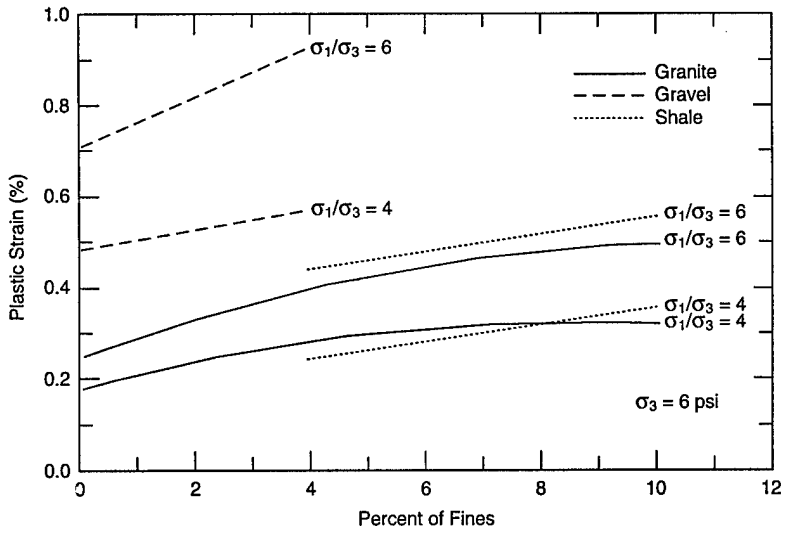

Figure 23. Influence of material type, stress level, and percent fines on plastic strain. (After Barksdale and Itani 1994.)

decreased by 50% (compared to the optimum moisture content) for river gravel at a bulk stress of 103 kPa. For undrained conditions, this reduction will be much higher. He also reported that the amount of fines in the base course materials had a significant effect on the amount of plastic strain (Fig. 23).

SUMMARY AND CONCLUSIONS

There are several methods for quantifying the shape, angularity, and roughness of base course aggregates. Methods developed by geologists can be classified as direct methods and involve actual measurements on the aggregates. Basic measurements of lengths are used to quantify the shape of aggregates. The angularity and roughness can also be determined with complex measurements, but several charts have been developed for simplifying the process. These methods are more involved and time consuming. However, they can be considered as standards.

Indirect methods for quantifying the shape, angularity, and roughness have been developed. The shape, angularity, and roughness are usually combined together as it is fairly difficult to separate the effects of the individual components. Most indirect measurements are based on the change in the voids of a single-sized bulk mass of aggregates. The tests are similar to one another and involve compaction of the aggregate mass in a given level. Some of the indices developed are the angularity number, particle index, and rugosity. Another index test involves the amount of time required for a given aggregate gradation to flow through a known orifice. This method is fairly simple and has been used for fine aggregates; it can be modified for coarse aggregates up to 50 mm in diameter.

Several research studies have shown that the shape, angularity, and roughness have a significant effect on base performance. Some of these studies have shown that there can be up to 50% change in resilient modulus of base materials due to geometric irregularities. It is not conclusive whether the resilient modulus is a good indication of the effects due to changes in shape, angularity, and roughness of the aggregates. However, what is clear in the literature is that moisture and amount of fines have a significant effect on base course performance. Increasing moisture content, as during the spring thaw, can increase the failure rate of the base course. Further study is needed to consider the combined effect of aggregate irregularities, moisture, and fines content on base course performance.

RECOMMENDATIONS

The results of this review indicate that for base course materials with maximum sizes ranging between 25 mm and 50 mm, the particle index test is best suited for indexing the angularity of the material. The term "angularity" as used in this recommendation includes the shape and surface characteristics of the aggregate. One of the drawbacks of using this test is that it is time consuming.

VAOT requirements state that any test method used for characterizing the angularity of base

course materials be simple and quick to use. Either the flow coefficient or the uncompacted void tests have the greatest potential to meet the above requirements. Currently, these tests are limited to aggregates with a maximum size of 20 mm, and modifications to both the equipment and test procedures are required. It is recommended that a research program be conducted to develop an index test for angularity of aggregates to a maximum size of 50 mm using both the flow coefficient and the uncompacted void tests. The results from both these tests will be correlated with the particle index, because this index has been developed for larger size aggregates.

It is also advisable, but optional, that the shape, angularity, and surface texture of the aggregates be characterized using the techniques developed in the geological arena. These will be used to calibrate the index results obtained from the flow coefficient and the uncompacted void tests using a similar method developed by Barksdale and Itani (1994). The geological characterization can also be used to correlate resilient modulus and shear strength test results using a similar approach used by Barksdale and Itani (1994) again.

The index angularity measurements need to be tied to the resilient and strength properties of the aggregates. Ideally, the resilient modulus and shear strength tests should be conducted under optimum moisture and saturated conditions. The critical time for the base courses in seasonal frost areas is during spring thaw. Therefore as a minimum it is recommended that the tests be conducted on saturated samples under undrained conditions. As a corollary to the testing program, moisture density relationships will be developed using the large-scale Proctor testing device. These relationships will be compared with those obtained from standard testing procedures used at VAOT.

LITERATURE CITED

Aldrich, R.C. (1996) Influence of aggregate properties on heavy duty pavements. Transportation Research Board.

ASTM D 2488-90 (1996) Standard practice for description and identification of soils (visual-manual procedure). *ASTM*, vol. 04.08, *Soil and Rock.*

ASTM D 3398-93 (1996) Standard test method for index of aggregate particle shape and texture. *ASTM*, vol. 04.03, *Road and Paving Materials.*

Barksdale, R.D., and S.Y. Itani (1994) Influence of aggregate shape on base behavior. Transportation Research Record 1227, p. 171–182.

Bikerman, J.J. (1964) Adhesion of asphalt to stone. MIT Civil Engineering, Research Report R64-3.

Bindra, S.P., and H.A. Al-Sanad (1983) Particle index evaluation of aggregates for unbound paving mixtures. In *Proceedings of the Fourth Conference of Road Engineering, 22–26 August.* Jakarta, Indonesia: Road Engineering Association of Asia and Australasia, p. 85–93.

British Standards Institution (1975) *BS 812: Testing Aggregates.*

Gupta, R.D. (1985) Effect of size of particles on their angularity. *Journal of the Institution of Engineers (India)*, **65**(CI 5): 210–214.

Holubec, I., and K.H. Wilson (1970) A cyclic creep study of pavement materials. Final Report, Department of Civil Engineering, University of Waterloo, Ontario, D.H.O. Report No. RR163.

Holtz, R.D., and W.D. Kovacs (1981) *An Introduction to Geotechnical Engineering.* Englewood Cliffs, New Jersey: Prentice-Hall, Inc.

Huang, E.Y. (1962) A test for evaluating the geometric characteristics of coarse aggregate particles. *Proceedings, American Society for Testing and Materials*, 62: 1223–1242.

Huang, E.Y. (1965) An improved particle index test for the evaluation of geometric characteristics of aggregate. Michigan Highway Research Project No. 86546.

Ishai, I., and H. Gelber (1982) Effect of geometric irregularity of aggregates on the properties and behavior of bituminous concrete. *Proceedings, Association of Asphalt Paving Technologists*, **51**: 494–521.

Ishai, I., and E. Tons (1971) Aggregate factors in bituminous mixture designs. University of Michigan, Ann Arbor, Report 335140-1-F.

Ishai, I., and E. Tons (1977) Concept and test method for a unified characterization of the geometric irregularity of aggregate particles. *Journal of Testing and Evaluation*, 5(1): 3–15.

Krumbein, W.C. (1941) Measurement and geological significance of shape and roundness of sedimentary particles. *Journal of Sedimentary Petrology*, **11**(2): 64–72.

Lees, G. (1964) The measurement of particle shape and its influence in engineering materials. *Journal of the British Granite and Whinestone Federation, London*, **4**(2): 1–22.

Lytton, R.L., J. Uzan, E.G. Fernando, R. Roque, D. Hiltunen, and S.M. Stoffel (1993) Development and validation of performance prediction models and specifications for asphalt binders and paving

mixes. Federal Highway Administration, Turner-Fairbanks Highway Research Center, Strategic Highway Research Program Report PA 357.

Rex, H.M., and R.A. Peck (1956) A laboratory test to evaluate the shape and surface texture of fine aggregate particles. *Public Roads*, **29**: 118–120.

Shergold, F.A. (1953) The percentage of voids in compacted gravel as a measure of its angularity. *Magazine of Concrete Research*, **5**(13): 3–10.

Sweere, G.T.H. (1990) Unbound granular bases for roads. Ph.D. Thesis, University of Delft.

Terzaghi, K., and R.B. Peck (1967) *Soil Mechanics in Engineering Practice*. New York: John Wiley and Sons, Second edition.

Thompson, M.R., and K.L. Smith (1990) Repeated triaxial characterization of granular bases. *Transportation Research Record*, **1278**: 7–17.

Tobin, R.E. (1978) Flow cone sand tests. *ACI Journal*, p. 1–12.

Tons E., and W.H. Goetz (1968) Packing volume concepts for aggregates. *Highway Research Record*, no. 236, p. 76–96.

Wadell, H. (1932) Volume, shape and roundness of rock particles. *Journal of Geology*, **40**: 443–451.

Wilson, J.D., L.D. Klotz, and C. Nagaraj (1995) Automated measurement of aggregate indices of shape. Federal Highway Administration Report FHWA-RD-95-116.

Witczak, M.W., and J. Uzan (1988) The universal airport pavement design system, Report I of IV: Granular material characterization. University of Maryland, College Park, Maryland.

Wright, P.J.F. (1955) A method of measuring the surface texture of aggregate. *Magazine of Concrete Research*, **7**(21): 151–160.

REPORT DOCUMENTATION PAGE

Form Approved
OMB No. 0704-0188

1. AGENCY USE ONLY (Leave blank)	2. REPORT DATE	3. REPORT TYPE AND DATES COVERED
	January 1998	

4. TITLE AND SUBTITLE

Quantification of Shape, Angularity, and Surface Texture of Base Course Materials

5. FUNDING NUMBERS

6. AUTHORS

Vincent Janoo

7. PERFORMING ORGANIZATION NAME(S) AND ADDRESS(ES)

U.S. Army Cold Regions Research and Engineering Laboratory
72 Lyme Road
Hanover, New Hampshire 03755-1290

8. PERFORMING ORGANIZATION REPORT NUMBER

Special Report 98-1

9. SPONSORING/MONITORING AGENCY NAME(S) AND ADDRESS(ES)

State of Vermont Agency of Transportation
133 State Street
Montpelier, Vermont 05602

10. SPONSORING/MONITORING AGENCY REPORT NUMBER

11. SUPPLEMENTARY NOTES For conversion of SI units to non-SI units of measurement consult *Standard Practice for Use of the International System of Units (SI)*, ASTM Standard E380-93, published by the American Society for Testing and Materials, 1916 Race St., Philadelphia, Pa. 19103.

12a. DISTRIBUTION/AVAILABILITY STATEMENT

Approved for public release; distribution is unlimited.

Available from NTIS, Springfield, Virginia 22161.

12b. DISTRIBUTION CODE

13. ABSTRACT (*Maximum 200 words*)

A state-of-the-art review was conducted to determine existing test methods for characterizing the shape, angularity, and surface texture of coarse aggregates. The review found direct methods used by geologists to determine these characteristics. These methods involve physical measurements of individual aggregates and are very laborious and time consuming. Engineers have developed index tests (indirect methods) to quantify the combined effect of the shape, angularity, and surface texture of coarse aggregates in terms of changes in the voids in the aggregate bulk. A description of both the direct and indirect methods is provided in the report. Also, the effect of shape, angularity, and surface texture of coarse aggregates on the base course performance was reviewed. It was found that there is some contradiction in the published data on resilient modulus. Shape, angularity, and surface texture of coarse aggregates clearly influence the angle of internal friction.

14. SUBJECT TERMS

Angularity
Coarse aggregates
Resilient modulus
Roughness
Shape

15. NUMBER OF PAGES
28

16. PRICE CODE

17. SECURITY CLASSIFICATION OF REPORT	18. SECURITY CLASSIFICATION OF THIS PAGE	19. SECURITY CLASSIFICATION OF ABSTRACT	20. LIMITATION OF ABSTRACT
UNCLASSIFIED	UNCLASSIFIED	UNCLASSIFIED	UL